


Diffusion of excitations and power-law localization in strongly disordered systems with long-range coupling

K. Kawa^{✉*} and P. Machnikowski^{✉†}

Department of Theoretical Physics, Wrocław University of Science and Technology, 50-370 Wrocław, Poland

 (Received 22 September 2020; revised 25 October 2020; accepted 26 October 2020; published 11 November 2020)

We investigate diffusion of excitation in one- and two-dimensional lattices with random onsite energies and deterministic long-range couplings (hopping) inversely proportional to the distance. Three regimes of diffusion are observed in strongly disordered systems: ballistic motion at short time, standard diffusion for intermediate times, and a stationary phase (saturation) at long times. We propose an analytical solution valid in the strong-coupling regime which explains the observed dynamics and relates the ballistic velocity, diffusion coefficient, and asymptotic diffusion range to the system size and disorder strength via simple formulas. We show also that in the long-time asymptotic limit of diffusion from a single site the occupations form a heavy-tailed power-law distribution.

DOI: [10.1103/PhysRevB.102.174203](https://doi.org/10.1103/PhysRevB.102.174203)

I. INTRODUCTION

The seminal paper of Anderson [1] anticipated lack of diffusion in particular random lattices in three dimensions (3D), starting the topic of Anderson localization of (quasi)particles. Although the original discussion concerned systems with power-law couplings, much of the subsequent research dealt with tight-binding-like models with nearest-neighbor coupling and onsite disorder. Within that framework, Mott and Twose [2] proved the lack of diffusion in one dimension (1D). Later, Abrahams *et al.* [3] proposed single parameter scaling hypothesis and proved the absence of diffusion in two dimensions (2D), confirming at the same time localization in one dimension and localization-delocalization phase transition in three dimensions with respect to the system size. Nonetheless, the single parameter scaling hypothesis remains an approximate result, demands finite range hopping, uncorrelated disorder and time-reversal symmetry. It still leaves space for the possibility of diffusion in specific models, even for dimension less or equal to two.

Beside the tight-binding model with onsite disorder and nearest-neighbor inter-site coupling, other theoretical models were studied from the point of view of localization and metal-insulator transition [4,5]. Among others, much interest was devoted to models of uncorrelated diagonal disorder with long-range hopping of the power-law character $\propto 1/r^\mu$ [4,6]. Such a model represents several physical systems. For instance, Levitov [7] analyzed delocalization of vibrational modes in a 3D crystal with dipole interaction $\propto 1/r^3$. Subsequently, the energy transfer in several systems has been explored extensively within similar models. In biological light-harvesting systems, energy transport to the reaction center is mediated by dipole interactions $\propto 1/r^3$ [8–10].

Furthermore, many-body systems of nuclear spins with the same $1/r^3$ interaction have been studied in the context of localization [11]. A model with both the short-range hopping between adjacent sites and long-range dipole-dipole coupling was used for describing energy transfer in self-assembled nanorings [12]. The long-range coupling was shown to stabilize the system against disorder. Moreover, energy transfer has been observed experimentally in the planar quantum dot (QD) ensembles [13]. It has been found that the transfer is even better for low-density samples, i.e., of greater inter-dot distances preventing carriers from tunneling between QDs. Thus, a mechanism different from quantum tunneling must be proposed for explaining the energy transfer, and a plausible explanation seems to be the long-range dipole-dipole coupling. In fact, an ensemble of QDs seems to be a coupled system, as its radiation properties cannot be explained as a sum of single emitters [14,15]. The fundamental coupling between the emitters emerges here from their interaction with a common electromagnetic reservoir, leading to the dispersion-force coupling $\propto \cos(kr)/(kr) + \sin(kr)/(kr)^2 + \cos(kr)/(kr)^3$ [16–18], where k is the resonant wave number, which reduces to the usual $1/r^3$ dipole interaction on short distances but is dominated by the $1/r$ term at distances larger than the wave length resonant with the optical transition.

A renormalization group analysis by Rodríguez *et al.* [4], proves the existence of extended states in the model of uncorrelated diagonal disorder and power-law hopping $\propto 1/r^\mu$, with an exponent μ greater than the dimension of the system. Extended states appear in such a system in the thermodynamic limit in the vicinity of the energy band edge, even in 1D and 2D. Such a model was also used for investigating the wave packet propagation in 1D [19]. Time evolution of the wave packet is described here by its mean square displacement and the participation ratio. The localization-delocalization transition occurs as a function of the disorder magnitude for $1 < \mu < 3/2$. For $\mu > 3/2$ wave packet tends to localize because of the short range of hopping decreasing while μ increases.

*Karol.Kawa@pwr.edu.pl

†Pawel.Machnikowski@pwr.edu.pl

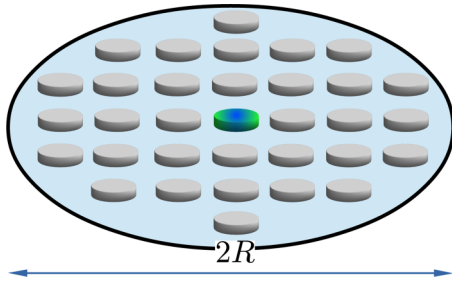


FIG. 1. The system geometry for $d = 2$: sites forming a regular lattice on a circular mesa. The initially excited site is marked by colors.

The particular case of $\mu = 1$, relevant to the dispersion forces at large distances and therefore corresponding to extended dipole-coupled natural (e.g., photosynthetic) or artificial (e.g., semiconductor) systems, shows interesting properties already in the absence of disorder, showing a combination of diffusive and super-diffusive transport [20]. However, in disordered systems this case has never been studied directly. Some of its features could only be inferred as a limit of the systematically studied case of $\mu > 1$. It is known, in particular, that it shows certain criticality features, like the divergence of the critical disorder strength needed to localize the upper band edge [21].

In this paper we consider the dynamics of a single excitation in arrays of two-level systems with exactly such long-range $1/r$ hopping and strong diagonal disorder. We show that a system of finite size in this limit shows three consecutive phases of excitation transport: a ballistic one, followed by normal diffusion, and finally saturation of the mean-square diffusion range. We analyze also the average distribution of the excitation in the asymptotic (saturation) phase and demonstrate a heavy-tail power-law quasilocalization around the initially excited site. We point out that in the strong disorder limit the excitation transfer is dominated by the direct coupling with the initial site, which allows us to reduce the model to a simplified form, which is exactly solvable in a certain range of parameters. In this way we are able to relate the transport parameters (ballistic speed, diffusion coefficient, and asymptotic diffusion range) to the system size and disorder strength.

The organization of the paper is as follows. In Sec. II, we describe the physical system and theoretical model. In Sec. III we present the results of our numerical simulations. The approximate analytical solution for strongly disordered systems is presented in Sec. IV A, analyzed in Sec. IV B, and discussed in Sec. IV C. Final conclusions are presented in Sec. V.

II. THE SYSTEM AND THE MODEL

In this section, we describe the physical system under study and introduce a theoretical model used for numerical simulation.

We study a d -dimensional ($d = 1, 2$) system of N sites on a regular lattice. The system occupies a disk of radius R for $d = 2$ and a line segment of length $2R$ for $d = 1$ (Fig. 1 shows the geometry for $d = 2$). The number of sites is related to

the dimensionless radius of the system (in units of the lattice constant) by $N = \zeta_d R^d$, where ζ_d is a number that depends on the space dimensionality d .

The system is described by the Hamiltonian

$$H = J \left(\sum_{\alpha} \epsilon_{\alpha} |\alpha\rangle \langle \alpha| + \sum_{\alpha\beta} V_{\alpha\beta} |\alpha\rangle \langle \beta| \right), \quad (1)$$

where $|\alpha\rangle$ represents a basis state localized at the site α , J sets the overall energy scale, $J\epsilon_{\alpha}$ is the corresponding onsite energy, and $JV_{\alpha\beta}$ is the coupling between the site states α and β . The dimensionless energies ϵ_{α} (in units of J) are uncorrelated normally distributed random variables of zero expected value and standard deviation σ . The coupling $V_{\alpha\beta}$ has a long-range character,

$$V_{\alpha\beta} = \begin{cases} \frac{1}{|\mathbf{r}_{\alpha} - \mathbf{r}_{\beta}|}, & \text{for } \alpha \neq \beta, \\ 0, & \text{for } \alpha = \beta, \end{cases} \quad (2)$$

where \mathbf{r}_{α} is the dimensionless position of the site α (in units of the lattice constant).

The central site is initially excited. The diffusion of the excitation is described by its mean square displacement (MSD) from the origin of the system

$$\langle r^2(t) \rangle = \left\langle \sum_{\alpha} |c_{\alpha}(t)|^2 r_{\alpha}^2 \right\rangle, \quad (3)$$

where $\langle \dots \rangle$ denotes the average over disorder realizations, $c_{\alpha}(t)$ are the coefficients of expansion of the system state in the localized basis,

$$|\Psi(t)\rangle = \sum_{\alpha} c_{\alpha}(t) |\alpha\rangle, \quad (4)$$

and the central site corresponds to the $\mathbf{r}_0 = \mathbf{0}$.

III. SIMULATION RESULTS

In this section we present the results of numerical simulations for the model described in Sec. II in one and two dimensions. The system evolution is found by exact numerical diagonalization of the system Hamiltonian. We investigate the character of the excitation diffusion as a function of the system parameters, i.e., the number of sites and the magnitude of the disorder characterized by its standard deviation σ . The MSD of the excitation from the central site is shown in Fig. 2 for different system sizes and disorder strengths. Three consecutive regimes of the excitation transport can be seen. First, the transport is ballistic with a certain velocity v ,

$$\langle r^2(t) \rangle = v^2 t^2, \quad \text{for } 0 < t < t_0. \quad (5)$$

The velocity depends on the system size, as can be seen in Figs. 2(a) and 2(b), but not on the disorder [Figs. 2(c) and 2(d)]. At a certain cross-over time t_0 , the normal diffusion with the diffusion coefficient D sets on

$$\langle r^2(t) \rangle = Dt, \quad \text{for } t_0 < t < t_1. \quad (6)$$

As demonstrated by our simulation results in Fig. 2, the diffusion coefficient D grows with the system size and decreases

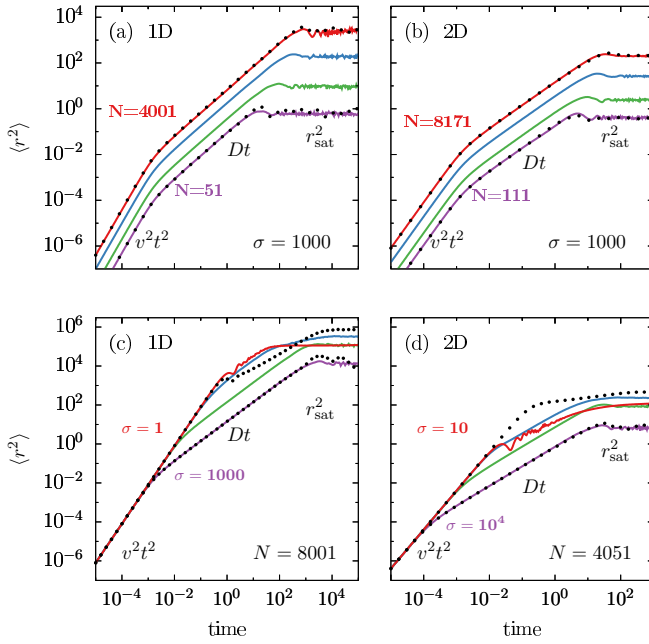


FIG. 2. The MSD of the excitation from the central site as a function of time: (a), (b) for different sizes of the system but the same disorder $\sigma = 1000$; (c), (d) for different disorder magnitudes but the same system sizes, as shown. Panels (a), (c) and (b), (d) show the results for $d = 1$ and $d = 2$, respectively. Dotted lines show the results from the “central atom model” (Sec. IV). All the results are averaged over 1000 repetitions.

as the disorder amplitude grows. From continuity requirement at the crossover one gets

$$t_0 = D/v^2. \quad (7)$$

Simulations show that this value is size-independent but increases with the disorder strength. Finally, saturation is reached at the second cross-over time t_1 ,

$$\langle r^2(t) \rangle = r_{\text{sat}}^2, \quad \text{for } t > t_1. \quad (8)$$

Obviously, the diffusion range must be limited in a finite system. However, the values of r_{sat}^2 presented in Fig. 2, although increasing with the number of nodes, are always considerably lower than the system size and decrease as the disorder grows. Again, the cross-over time is fixed by continuity,

$$t_1 = r_{\text{sat}}^2/D. \quad (9)$$

To study the dependence of the dynamical characteristics v , D , and r_{sat}^2 on the system size and disorder strength, we found the system evolution for a range of values of N and σ , and fitted the numerical solutions in the respective time intervals with the appropriate power-law functions of time according to Eqs. (5), (6), and (8). The dependence of all the dynamical characteristics on the two system parameters turns out to be a power law over at least a decade of parameter variation in each case, with the power-law exponent very close to an integer or a simple fraction.

The size dependence of the velocity and diffusion coefficient is depicted in Figs. 3(a) and 3(b). The velocity increases with the number of atoms like $N^{1/2}$, while the diffusion coefficient grows linearly with the number of sites both in 1D

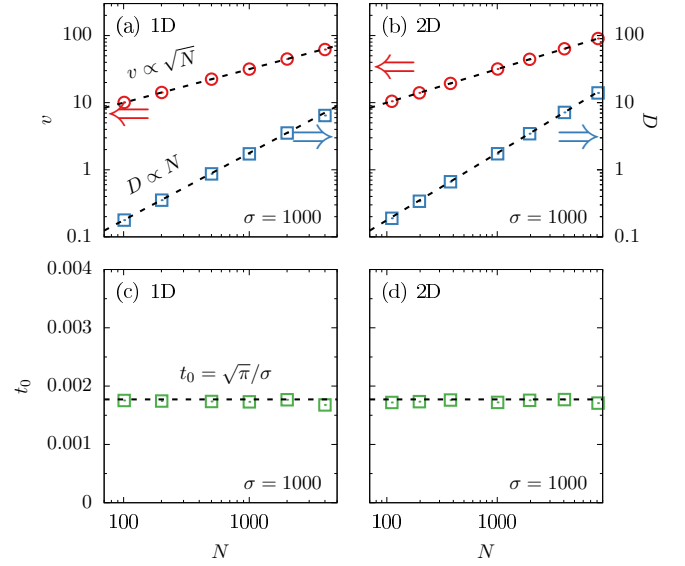


FIG. 3. Size dependence of the dynamical coefficients. (a), (b) The ballistic velocity (green circles, right axis) and the diffusion coefficient (red squares, left axis) as a function of the number of sites. (c), (d) The ballistic-to-diffusive crossover time as a function of the number of sites. Lines show the analytical results from the “central atom model” [see Eqs. (24)–(26) in Sec. IV B].

and 2D. As a consequence [Eq. (7)], the first cross-over time is size independent, see Figs. 3(c) and 3(d).

The dependence of the dynamical parameters on the disorder strength is shown in Figs. 4(a) and 4(b). While the velocity remains σ -independent, as already concluded above,

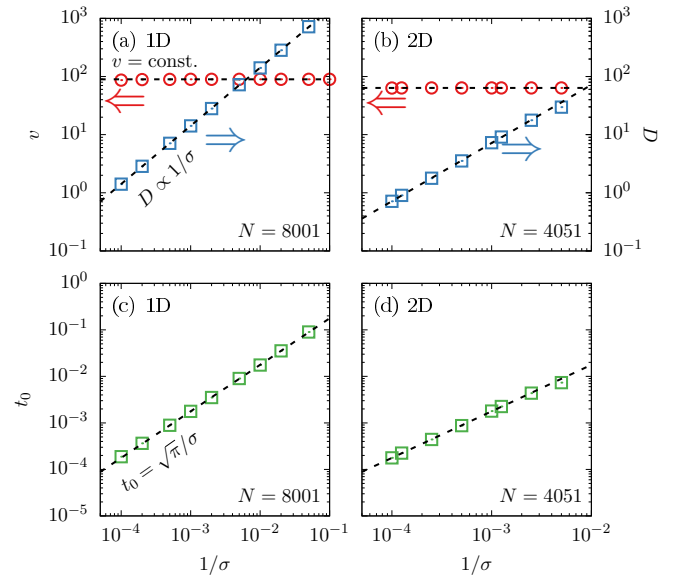


FIG. 4. Dependence of the dynamical coefficients on the disorder strength. (a), (b) The ballistic velocity (red circles, left axis) and the diffusion coefficient (blue squares, right axis) as a function of the standard deviation of the onsite energies. (c), (d) The ballistic-to-diffusive crossover time as a function of the standard deviation of the onsite energies. Lines show the analytical results from the “central atom model” [see Eqs. (24)–(26) in Sec. IV B].

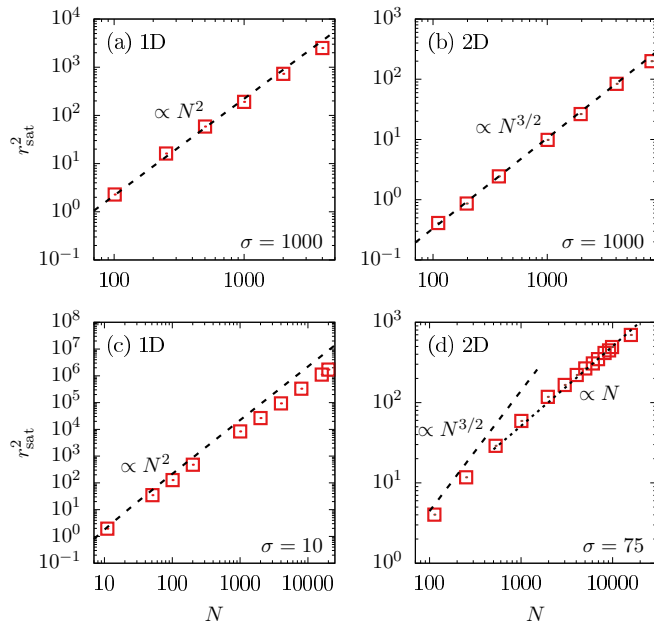


FIG. 5. The dependence of the diffusion range on the number of sites in one (a), (c) and two (b), (d) dimensions. Dashed lines show the analytic results from the “central atom model” [see Eq. (27) in Sec. IV B]. Dotted line in (d) is the linear fit to the further part of the plot.

the diffusion coefficient is inversely proportional to σ for any system dimension.

Finally, in Figs. 5 and 6 we analyze the dependence of the saturation level r_{sat}^2 on the system size and disorder strength, respectively. In 1D, the value of r_{sat}^2 grows as N^2 for large disorder [Fig. 5(a)], while for moderate disorder one observes an approximately power-law dependence with a lower exponent [Fig. 5(c)]. In 2D the dependence is $r_{\text{sat}}^2 \propto N^{3/2}$ for strongly disordered systems [Fig. 5(b)] and for sufficiently short chains at weaker disorder [Fig. 5(d)]. This kind of power-law dependence in two dimensions means that the saturation level grows faster than the system size, hence the excitation must reach the border of the system for sufficiently large number of sites (on the order of σ^2). From that point saturation level starts to

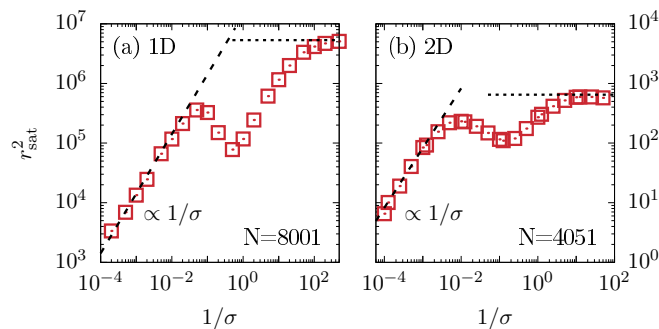


FIG. 6. The dependence of the diffusion range on the standard deviation of the onsite energies in one (a) and two (b) dimensions. Solid lines show the analytical results from the “central atom model” [see Eq. (27) in Sec. IV B]. Dotted lines represent the values corresponding to uniform distribution over the system.

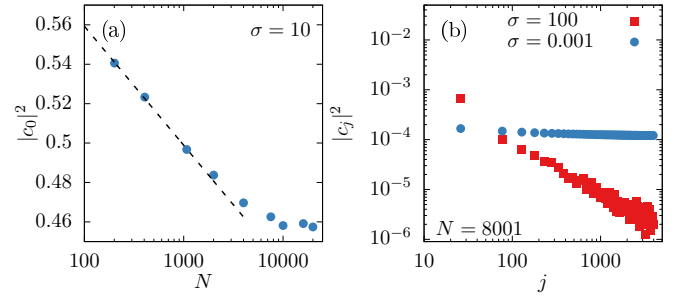


FIG. 7. (a) The final (long-time asymptotic) occupation of the initial site in a one-dimensional chain as a function of the chain length for $\sigma = 10$. (b) The dependence of the asymptotic occupation on the site index in a one-dimensional chain for the values of N and σ as shown. The dashed line shows a logarithmic trend.

grow linearly with the system size as it is clear from Fig. 5(d). In other words, the saturation level is bounded by the system size. Both in 1D and 2D, the value of r_{sat}^2 turns out to be proportional to $1/\sigma$ as long as $\sigma \gg 1$, while it starts to oscillate and reaches a constant value as $\sigma \rightarrow 0$. The latter property simply reflects the uniform spreading of the excitation across the system, characteristic of an unperturbed lattice, which roughly sets the upper limit on the mean-square displacement. The values corresponding to the uniform distribution are $R^2/3$ and $R^2/2$ for $d = 1$ and $d = 2$, respectively, and are marked with horizontal dotted lines in Fig. 6. The crossover time t_1 is then proportional to N and $N^{1/2}$ in 1D and 2D respectively, that is, to the linear size of the system in both cases, and is independent of disorder, as follows from Eq. (9).

By a simple lowest-order “resonance counting” argument, the number of sites resonant to the central (initially occupied) one at a distance x is proportional to $1/x$. For a 1D system, as the chain gets longer, due to occupation spreading among these resonant sites, the occupation of the distant sites would then grow as $\ln N$, the value of r_{sat}^2 would grow as N^2 , and the long-time occupations would be distributed as $1/x$. This prediction for r_{sat}^2 agrees with the simulation results for very large disorder but discrepancy is visible at $\sigma = 10$ [Fig. 5(c)]. The growing occupation of the distant sites should suppress the final occupation of the initial site $|c_0|^2$ (the survival probability) as $1 - A \ln N$, until the survival probability is reduced enough for the lowest order approach to break down. This is indeed confirmed by simulation results presented in Fig. 7(a), where the logarithmic dependence is represented by the dashed trend line, although the narrow range of variability of $|c_0|^2$ may be insufficient to rigorously prove the subtle logarithmic dependence. The saturation at $N \gtrsim 10^4$ appears at a rather high value of the survival probability. The distribution of occupations at saturation (asymptotic long-time limit) indeed shows a distinct power-law character over many orders of magnitude of the chain length, with an exponent very close to 1 for strong disorder [red squares in Fig. 7(b)]. This behavior is characteristic of the strong disorder regime, corresponding to the power-law dependence of r_{sat}^2 on σ [left asymptotics of Fig. 6(a)]. It should be contrasted with the low-disorder limit [right asymptotics in Fig. 6(a)], where the occupations are equally spread all over the chain, as we have already inferred from the asymptotic value [blue circles in Fig. 7(b)].

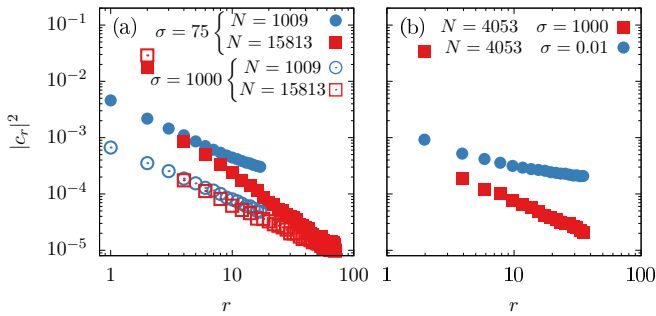


FIG. 8. The dependence of the asymptotic occupation on the distance from the initially occupied site in a two-dimensional system: (a) for a fixed σ and two values of N as shown; (b) for a fixed N and two values of σ as shown.

A similar power-law localization of the asymptotic state is observed in a 2D system, as shown in Fig. 8, where we plot the average occupation of a site as a function of its distance from the central site. As can be seen in Fig. 8(a) (full symbols), for a moderate disorder strength, the exponent of this power-law dependence increases by magnitude as the system size grows. The values from fitting to the power-law part of the data obtained from simulations range from -1.0 for $N = 197$ to -1.7 for $N = 32017$ (fitting was performed using the central part of the data points, showing the clear power-law dependence and may be slightly affected by the choice of the cutoffs). All these values are above -2 and therefore correspond to heavy tail distributions in two dimensions that would have a divergent norm if extrapolated to infinite size. The values seem to be roughly proportional to $\ln N$ over the range of system sizes available for numerical simulations and we were not able to reliably determine the asymptotic value of the exponent as $N \rightarrow \infty$.

A different situation is observed for strongly disordered systems [empty symbols in Fig. 8(a)]. Here the slope of the power-law dependence is apparently constant and indeed, the exponents obtained from fitting oscillate (due to inherent randomness and fitting uncertainty) very close to the value of -1 , which precisely corresponds to the $r_{\text{sat}}^2 \propto N^{3/2}$ dependence in Fig. 5(b). This means that in this range of system sizes, the asymptotic diffusion range grows with the system size by extending the $\propto 1/r$ dependence of occupation to larger and larger distances at the cost of the central site occupation, until the $\propto N^{3/2}$ dependence breaks down, similar to the situation in Fig. 5(d) but far beyond the range of system sizes accessible in simulations. When comparing the power-law dependence at the two disorder strengths one arrives at the somewhat unexpected conclusion that, from the formal point of view focused merely on the power-law exponent, localization in moderately disordered systems is stronger (the absolute value of the exponent is larger) than in heavily disordered ones. This is obviously not true in terms of the actual values of the occupations that decrease as the disorder grows, which simply means that the survival probability at the initial site grows with disorder, as expected. Interestingly, the occupations of the most remote sites are similar for the two different disorder regimes shown in Fig. 8(a).

The trend in the dependence of the average asymptotic distribution of occupations on the disorder strength demonstrated above cannot remain valid toward weaker disorder strengths, as the occupation should spread across all the system in the limit of unperturbed chain. Indeed, as shown in Fig. 8(b), for a very weak disorder, the system tends to a uniform distribution but, rather surprisingly, even for $\sigma = 0.01$ a weak localization effect is still visible.

In addition to the simulations of the full model discussed so far, we have also studied the dynamics of a “central atom model” in which the central (initially excited) site is coupled to all the other sites in the system as in the full model, but the other sites are not coupled with one another, i.e., $V_{\alpha\beta} = 0$ if $\alpha \neq 0$ and $\beta \neq 0$. The results are shown in Fig. 2 with dotted lines. One can see that the system evolution is nearly the same in both models in this parameter range, which means that the dynamics in the strongly disordered case is dominated by direct jumps to remote places, which is possible due to the long-range coupling.

In the next section we show that the dynamical parameters can be related to the system size and disorder strength and the analytical relation between the power-law exponents and the system dimension can be found as long as the “central atom model” is valid.

IV. APPROXIMATE ANALYTICAL SOLUTION

In this section we present an approximate analytic approach to the considered problem, which becomes possible within the simplified “central atom model” in the limit of strong disorder.

A. Solution of the equation of motion

The equation of motion for the coefficients of the expansion defined in Eq. (4) has the form

$$i\dot{c}_\alpha(t) = \epsilon_\alpha c_\alpha(t) + \sum_{\beta} V_{\alpha\beta} c_\beta(t), \quad c_\alpha(0) = \delta_{\alpha 0}. \quad (10)$$

We define the Laplace transform $f_\alpha(s)$ of an amplitude $c_\alpha(t)$,

$$f_\alpha(s) = \int_0^\infty e^{-st} c_\alpha(t) dt, \quad (11)$$

where s is a complex variable. Equation (10) in terms of the Laplace transform is

$$f_\alpha(s) = \frac{i\delta_{0\alpha}}{is - \epsilon_\alpha} + \sum_{\beta \neq \alpha} \frac{V_{\alpha\beta}}{is - \epsilon_\alpha} f_\beta(s). \quad (12)$$

Equation (12) can be iteratively expanded in series depending only on the central-site term f_0 ,

$$f_\alpha(s) = \frac{V_{\alpha 0}}{is - \epsilon_\alpha} f_0(s) + \sum_{\beta \neq \alpha, \beta \neq 0} \frac{V_{\alpha\beta}}{is - \epsilon_\beta} \frac{V_{\beta 0}}{is - \epsilon_\beta} f_0(s) + \dots, \quad \alpha \neq 0 \quad (13)$$

and

$$f_0(s) = \frac{1}{is - \epsilon_0} + \left[\sum_{\beta \neq 0} \frac{V_{0\beta} V_{\beta 0}}{(is - \epsilon_0)(is - \epsilon_\beta)} + \sum_{\gamma \neq \beta, \gamma \neq 0} \frac{V_{0\beta} V_{\beta\gamma} V_{\gamma 0}}{(is - \epsilon_0)(is - \epsilon_\beta)(is - \epsilon_\gamma)} + \dots \right] f_0(s). \quad (14)$$

The series have the number of terms of the order of N^N and the resulting system of equations cannot be solved in a simple manner. The problem simplifies considerably in the ‘‘central atom approximation.’’ Then, only the first term in Eq. (13) remains, while in Eq. (14) only the first term and the first sum survive. After these simplifications, one can write $f_\alpha(s)$ as

$$f_\alpha(s) = \frac{iV_{\beta 0} \prod_{\beta \neq 0, \beta \neq \alpha} (is - \epsilon_\beta)}{\prod_{\beta} (is - \epsilon_\beta) - \sum_{\beta \neq 0} \prod_{\gamma \neq \beta, \gamma \neq 0} V_{0\beta} V_{\beta 0} (is - \epsilon_\gamma)}. \quad (15)$$

Next, we transform back to the time domain, by means of the Mellin’s formula

$$c_\alpha(t) = \frac{1}{2\pi i} \lim_{T \rightarrow \infty} \int_{\gamma - iT}^{\gamma + iT} e^{st} f_\alpha(s) ds. \quad (16)$$

To perform the integral we employ residue theorem and obtain

$$c_\alpha(t) = \sum_n b_n^{(\alpha)} e^{-iz_n t}, \quad (17)$$

where $z_n = is_n$ and s_n are the poles of the analytic function given by Eq. (15). All z_n must be real. In addition,

$$b_n^{(\alpha)} = 2\pi i \text{Res}_{z_n} f_\alpha(z) = \frac{V_{\alpha 0} \prod_{\beta \neq 0, \beta \neq \alpha} (z_n - \epsilon_\beta)}{\prod_{\beta \neq n} (z_n - z_\beta)}, \quad (18)$$

where $\text{Res}_{z_n} f_\alpha(z)$ denotes the residue of $f_\alpha(z)$ at z_n .

As long as the coupling is small in comparison to σ/N , the roots of the denominator of Eq. (15) lie in close vicinity to bare energies ϵ_α , as compared to the typical distance between these roots. Hence, one can associate each pole with the nearest bare energy, align the numbering and assume $\frac{z_n - \epsilon_\beta}{z_n - z_\beta} \approx 1$, whenever $n \neq \beta$. With this approximation, one finds

$$b_n^{(\alpha)} \approx \begin{cases} \frac{V_{\alpha 0}}{z_0 - z_\alpha}, & n = 0, n \neq \alpha, \\ \frac{V_{\alpha 0}}{z_n - z_0}, & n = \alpha \neq 0, \\ 0, & \text{otherwise.} \end{cases}$$

The amplitudes $c_\alpha(t)$ then take the form

$$c_\alpha(t) = b_0^{(\alpha)} e^{-iz_0 t} + b_\alpha^{(\alpha)} e^{-iz_\alpha t} = e^{-iz_0 t} \frac{V_{\alpha 0}}{z_0 - z_\alpha} [1 - e^{-i(z_0 - z_\alpha)t}]$$

and the occupation of the site α becomes

$$|c_\alpha(t)|^2 = |V_{\alpha 0}|^2 \frac{\sin^2(\delta z_\alpha t/2)}{(\delta z_\alpha/2)^2}, \quad (19)$$

where $\delta z_\alpha = z_0 - z_\alpha$. Upon inserting this result to the Eq. (3) we obtain

$$\langle r^2(t) \rangle = \left\langle \sum_r r^2 |V_r|^2 \sum_{k=1}^{n_r} \frac{\sin^2(\delta z_k(r)t/2)}{[\delta z_k(r)/2]^2} \right\rangle, \quad (20)$$

where we decomposed the sum over all the sites into subsets of n_r sites lying at a distance r from the origin. All the sites at a given distance have the same coupling to the central dot $V_r = 1/r$. $\delta z_k(r)$ are the values of δz_k for sites lying at distance r from the origin. $\delta z(r)$ can be considered random variables with a certain probability density $f_r(\delta z)$. In the continuum approximation one then obtains

$$\langle r^2(t) \rangle = \int_0^R \zeta_d r^{d-1} dr \int_{-\infty}^{\infty} f_r(u) \frac{\sin^2(ut/2)}{(u/2)^2} du, \quad (21)$$

where $\zeta_d r^d$ is the number of sites lying inside a d -dimensional sphere.

At large δz , the poles are shifted negligibly from the bare energies, hence the distribution function is close to the onsite energy difference distribution $f_\infty(\delta\epsilon)$ (here ∞ refers to infinite distance, hence vanishing coupling, and $\delta\epsilon$ is the bare energy difference), which is a Gaussian distribution with the standard deviation $\sqrt{2}\sigma$. However, at $\delta z \sim V_r$ the pole probability distribution must reflect the level repulsion. Its form can be found by noting that a pair of sites with a bare energy difference $\delta\epsilon > 0$ coupled with a coupling strength V gives rise to a pair of poles separated by $\delta z = \sqrt{(\delta\epsilon)^2 + 4V^2}$. From this, the cumulative distribution function for δz follows in the form

$$P(0 < \delta z_k(r) < u) = \int_0^{\sqrt{u^2 - 4V_r^2}} f_\infty(x) dx, \quad |u| > 2V_r, \quad (22)$$

and the corresponding probability density is

$$f_r(u) = \begin{cases} f_\infty(\sqrt{u^2 - 4V_r^2}) \frac{|u|}{\sqrt{u^2 - 4V_r^2}}, & |u| > 2V_r, \\ 0, & |u| \leq 2V_r. \end{cases} \quad (23)$$

The above distribution corresponds to the normal distribution of standard deviation $\sigma_u = \sqrt{2}\sigma$ having a gap around zero of width $4V_r$. The total distribution for a system of radius R including all possible distances r has a gap of width $4V_R$.

B. Regimes of propagation

Equations (21) and (23) allow us to explain the three time phases in the excitation evolution.

For very short times, $t \lesssim 1/\sigma$, the function $h(u) = \sin^2(ut/2)/(u/2)^2$ is slowly varying in u and can be approximated by $h(u) \approx t^2$ over the whole width of the distribution $f_r(u)$, as schematically shown in Fig. 9(a). Equation (21) then immediately yields $\langle r^2(t) \rangle = v^2 t^2$, that is, ballistic propagation with the constant velocity

$$v^2 = \int_0^R \zeta_d r^{d-1} dr \int f_\infty(u) du = \zeta_d R^d = N. \quad (24)$$

This dependence is shown as dashed lines in Figs. 3(a) and 3(b), which perfectly follows the numerical data.

In the intermediate time range, $1/\sigma < t < 1/V_R$, the function $h(u)$ probes the central part of the distribution but is still

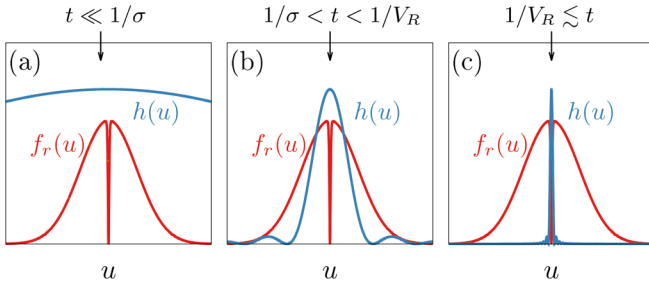


FIG. 9. Schematic plots of the probability density f_r (red, the same for three cases) and the function $h(u)$ (blue) corresponding to three phases of propagation: (a) ballistic, (b) diffusive, (c) saturation.

insensitive to the narrow central gap [Fig. 9(b)]. Then the integral over u in Eq. (21) can be approximated by

$$\begin{aligned} & \int_{-\infty}^{\infty} f_r(u) \frac{\sin^2(ut/2)}{(u/2)^2} du \\ & \approx \int_{-\infty}^{\infty} f_{\infty}(u) 2\pi t \delta(u) du = 2\pi t f_{\infty}(0), \end{aligned}$$

from which one finds the diffusive transport $\langle r^2(t) \rangle = Dt$, with

$$D = \int_0^R dr \zeta_d r^{d-1} 2\pi t f_{\infty}(0) = \frac{\sqrt{\pi} N}{\sigma}. \quad (25)$$

Again, this dependence on N and σ is shown as dashed lines in Figs. 3(a) and 3(b) and in Figs. 4(a) and 4(b). The agreement with the numerical data is excellent.

Using Eq. (7), the crossover time between ballistic and diffusive phases is obtained as

$$t_0 = \sqrt{\pi}/\sigma, \quad (26)$$

which agrees with our simulation results, as shown in Figs. 4(c) and 4(d), for sufficiently large values of σ . The range of the ballistic transport is therefore $\langle r^2(t_0) \rangle = v^2 t_0^2 = N\sqrt{\pi}/\sigma$. In 1D it is always much smaller than the system size if the disorder is strong.

Finally, at $t \approx 1/V_R$, the function $h(u)$ becomes as narrow as the the gap in the density function, hence its central part does not contribute, while its oscillating tails are averaged to $\tilde{h}(u) = (1/2)/u^2$ (see Fig. 9). There is no time dependence in this limit, which results in the saturation of $\langle r^2 \rangle$. The saturation level is then estimated from Eq. (21) as $2 \int_{V_r}^{\infty} f_r(u) \tilde{h}(u) du = \frac{\sqrt{\pi} r}{2\sigma} \exp[1/(\sigma^2 r^2)] \operatorname{erfc}[1/(\sigma r)]$. The resulting saturation value is

$$\begin{aligned} r_{\text{sat}}^2 = \langle r^2(t) \rangle &= \int_0^R \zeta_d dr^d \frac{\sqrt{\pi}}{2\sigma} \exp\left(\frac{1}{\sigma^2 r^2}\right) \operatorname{erfc}\left(\frac{1}{\sigma r}\right) dr \\ &\approx \frac{\sqrt{\pi} \zeta_d}{2\sigma} \frac{d}{d+1} R^{d+1}, \end{aligned} \quad (27)$$

where we took into account that $V_R/\sigma = 1/R\sigma \ll 1$ in the high disorder energy regime, so the last two terms in the integral tends to unity (in the zeroth order of Taylor expansion).

The dependence from Eq. (27) is marked by dashed lines in Figs. 5 and 6 and agrees very well with the simulation result as long as the size is not too large and the disorder is strong.

The onset of saturation is determined by the continuity of $\langle r^2 \rangle$, $Dt_1 = r_{\text{sat}}^2$. Combining Eqs. (27) with (25), one obtains

$$t_1 = \frac{1}{\pi V_R}, \quad (28)$$

in agreement with the simulations.

Within the ‘‘central atom model,’’ the asymptotic occupation of a site at a distance r from the origin is

$$\begin{aligned} \langle |c_r|^2 \rangle_{\text{sat}} &= \frac{2}{r^2} \int_{2V_r}^{\infty} f_r(u) \frac{2}{u^2} du \\ &= \frac{\sqrt{\pi}}{2\sigma r} \exp\left(\frac{1}{\sigma^2 r^2}\right) \operatorname{erfc}\left(\frac{1}{\sigma r}\right) \approx \frac{\sqrt{\pi}}{2\sigma r}. \end{aligned} \quad (29)$$

This $\propto 1/r$ trend obtained from our approximate analytical solution agrees with the numerical data in 1D, shown in Fig. 7 and corresponds to the survival probability $1 - A \ln N$ in the strong disorder regime, which is consistent with the simulation data in Fig. 7(a). In 2D, as we have seen in Fig. 8, the same dependence is obtained for very strongly disordered systems.

C. Discussion

As we have seen, the analytical formulas agree very well with the simulation results only within a certain limits of system size and disorder strength. One discrepancy appears when the disorder becomes weak (see Fig. 6). This is obvious, as our ‘‘central atom model’’ is essentially based on the assumption that coupling is a perturbation to the onsite energies, which requires a strong disorder. The second discrepancy appears for long chains in Fig. 5. For $d \geq 2$, $r_{\text{sat}}^2 \sim R^{d+1}$, Eq. (27) predicts that the asymptotic diffusion range grows faster than the system size. This cannot be true for an arbitrary system size and, indeed, the trend in simulations changes at a certain system size Fig. 5(d), which is not captured by the ‘‘central atom’’ approximation. We note that the limit of validity of our approximation is $\sigma/N \sim V_R = 1/R$ or, using $N \sim R^d$, $R^{d-1} \sim \sigma$. At this limit, $\langle r_{\text{sat}}^2 \rangle \sim R^2$, which assures consistency of our conclusions. However, for a one-dimensional chain, $r_{\text{sat}}^2 \sim R^2$, hence the asymptotic range grows linearly with the system size. Eq. (27) is valid for $\sigma \gg 1$, hence $r_{\text{sat}}^2 \ll R^2$ and the excitation is effectively trapped around the original site in the chain.

V. CONCLUSIONS

We have studied the diffusion of an initially localized excitation in finite lattices with a strong onsite disorder and a long-range coupling (hopping) inversely proportional to the distance. We have shown that the diffusion in such a system takes place in three dynamical stages: ballistic transport is followed by normal diffusion and then by saturation. The numerical findings can be understood with the help of an approximate model which is valid in the strong disorder regime and allows an analytical solution, which relates the dynamical properties to the system parameters (size and disorder strength).

We have proposed two complementary descriptions of localization. The first one emerges from the dynamics and consists in analyzing the asymptotic range of diffusion. The

other one consists in studying the spatial distribution of the average occupations of lattice sites in the long-time limit and is more directly related to the structure of energy eigenstates of the disordered system. We have shown, both numerically and analytically, that the diffusion range grows proportionally to the system size and is always much smaller than the latter in 1D hence, from this point of view, the excitation remains effectively localized around the initial site. In contrast, in 2D systems, the range of diffusion initially grows faster than the system size as the latter increases, until at a certain system size the growth slows down so that, in sufficiently strongly disordered systems the range again remains much smaller than the system size. While tracing the asymptotic diffusion range provides only a single number characterizing the degree of localization or spreading of the excitation, inspection of the average profile of occupations offers a more complete spatial picture of the localization. We have found out that

after a sufficiently long time the occupations stabilize into a heavy-tailed power-law distribution both in 1D and 2D that not only does not have a second moment but would even have a divergent norm when extrapolated to infinite system size. Therefore, even if the excitation remains localized in the sense of showing the diffusion range much smaller than the system size, it does not have any intrinsic localization length and the diffusion reaches (on the average) an arbitrary site of the lattice according to the power-law distribution as a function of the distance.

ACKNOWLEDGMENTS

The authors are grateful to Marcin Mierzejewski for discussions. Calculations have been partially carried out using resources provided by Wrocław Centre for Networking and Supercomputing [22], Grant No. 203.

-
- [1] P. W. Anderson, *Phys. Rev.* **109**, 1492 (1958).
 - [2] N. Mott and W. Twose, *Adv. Phys.* **10**, 107 (1961).
 - [3] E. Abrahams, P. W. Anderson, D. C. Licciardello, and T. V. Ramakrishnan, *Phys. Rev. Lett.* **42**, 673 (1979).
 - [4] A. Rodríguez, V. A. Malyshev, G. Sierra, M. A. Martín-Delgado, J. Rodríguez-Laguna, and F. Domínguez-Adame, *Phys. Rev. Lett.* **90**, 027404 (2003).
 - [5] G. Roati, C. D’Errico, L. Fallani, M. Fattori, C. Fort, M. Zaccanti, G. Modugno, M. Modugno, and M. Inguscio, *Nature* **453**, 895 (2008).
 - [6] F. Domínguez-Adame and V. Malyshev, *Am. J. Phys.* **72**, 226 (2004).
 - [7] L. S. Levitov, *Europhys. Lett.* **9**, 83 (1989).
 - [8] G. L. Celardo, F. Borgonovi, M. Merkli, V. I. Tsifrinovich, and G. P. Berman, *J. Phys. Chem. C* **116**, 22105 (2012).
 - [9] M. Sarovar, A. Ishizaki, G. R. Fleming, and K. B. Whaley, *Nat. Phys.* **6**, 462 (2010).
 - [10] M. Mohseni, P. Rebentrost, S. Lloyd, and A. Aspuru-Guzik, *J. Chem. Phys.* **129**, 174106 (2008).
 - [11] G. A. Álvarez, D. Suter, and R. Kaiser, *Science* **349**, 846 (2015).
 - [12] A. D. Somoza, K. W. Sun, R. A. Molina, and Y. Zhao, *Phys. Chem. Chem. Phys.* **19**, 25996 (2017).
 - [13] F. V. De Sales, S. W. Da Silva, J. M. Cruz, A. F. Monte, M. A. Soler, P. C. Morais, M. J. Da Silva, and A. A. Quivy, *Phys. Rev. B* **70**, 235318 (2004).
 - [14] M. Scheibner, T. Schmidt, L. Worschech, A. Forchel, G. Bacher, T. Passow, and D. Hommel, *Nat. Phys.* **3**, 106 (2007).
 - [15] M. Kozub, L. Pawicki, and P. Machnikowski, *Phys. Rev. B* **86**, 121305(R) (2012).
 - [16] M. J. Stephen, *J. Chem. Phys.* **40**, 669 (1964).
 - [17] R. H. Lehmberg, *Phys. Rev. A* **2**, 883 (1970).
 - [18] A. A. Varfolomeev, *Zh. Eksp. Teor. Fiz.* **59**, 1702 (1970).
 - [19] P. E. De Brito, E. S. Rodrigues, and H. N. Nazareno, *Phys. Rev. B* **69**, 214204 (2004).
 - [20] B. Kloss and Y. Bar Lev, *Phys. Rev. A* **99**, 032114 (2019).
 - [21] F. A. B. F. de Moura, A. V. Malyshev, M. L. Lyra, V. A. Malyshev, and F. Domínguez-Adame, *Phys. Rev. B* **71**, 174203 (2005).
 - [22] <http://wcss.pl>.